Universal pulse shape scaling function and exponents: Critical test for avalanche models applied to Barkhausen noise

Amit P. Mehta,[1] Andrea C. Mills,[1] Karin A. Dahmen,[1] and James P. Sethna[2]
[1]*Department of Physics, University of Illinois at Urbana-Champaign, Urbana, Illinois 61801*
[2]*Laboratory of Atomic and Solid State Physics (LASSP), Clark Hall, Cornell University, Ithaca, New York 14853*
(Received 7 December 2001; published 10 April 2002)

In order to test if the universal aspects of Barkhausen noise in magnetic materials can be predicted from recent variants of the nonequilibrium zero-temperature Random Field Ising Model, we perform a quantitative study of the universal scaling function derived from the Barkhausen pulse shape in simulations and experiment. Through data collapses and scaling relations we determine the critical exponents τ and $1/\sigma\nu z$ in both simulation and experiment. Although we find agreement in the critical exponents, we find differences between theoretical and experimental pulse shape scaling functions as well as between different experiments.

DOI: 10.1103/PhysRevE.65.046139 PACS number(s): 64.60.Ht, 75.60.−d, 72.70.+m

I. INTRODUCTION

Real materials have dirt or disorder, which often leads to slow (glassy) dynamics due to complex free energy landscapes with diverging energy barriers [1]. On long length scales and practical time scales, thermal effects often become unimportant. Indeed, when such a system is driven by an external field it jumps from one local metastable free energy minimum to the next, and the state of the system depends on its history.

In magnetic materials jumps from one local minimum to the next involve a collective process whereby clusters of magnetic domains change the direction of their magnetization, in an avalanche. These avalanches can be triggered by a slowly but continuously increasing homogeneous external magnetic field H (taken from $-\infty$ to $+\infty$). These avalanches produce so-called Barkhausen noise, which can be observed experimentally as a voltage signal induced in a pickup coil wound around the magnet. Experiments show that these avalanches come in all sizes; their sizes are typically distributed according to a power law over several decades. Other systems also exhibit a broad range of avalanche sizes and durations following power laws: superconducting vortex line avalanches [2], resistance avalanches in a superconducting film [3], capillary condensation of helium in Nuclepore [4], acoustic emissions in athermal martensites [5], earthquakes [6], and many others [7].

We examine two variants of the nonequilibrium zero-temperature random field Ising model (RFIM), which both predict power law distributions of avalanche sizes and *universal* nonequilibrium collective behavior. The RFIM is a model for a conventional magnet in which magnetic domains are modeled by ''spins'' on a lattice that can only point up or down. The first variant basically exhibits single front (domain wall) propagation dynamics in which spins at the edge of an existing front flip when it is (locally) energetically favorable to do so. Spins that are not adjacent to this front are very unlikely to flip on their own due to the presence of an infinite-range demagnetizing field, which is present in addition to nearest neighbor ferromagnetic interactions. We call this the front propagation model [8]. In the second variant, called the nucleation model, spins flip anywhere in the system when it is (locally) energetically favorable to do so. In this case there are *many interacting* fronts, unlike in the front propagation model. Only nearest neighbor ferromagnet interactions are included in the nucleation model [9].

In this paper we perform a detailed quantitative comparison of the universal avalanche pulse shapes and exponents obtained from: front propagation dynamics, domain nucleation dynamics, and experiment. Our analysis constitutes a test of whether the nonequilibrium zero-temperature RFIM (either variant) is in the same universality class as experimental systems exhibiting Barkhausen noise.

II. THE MODEL

The RFIM consists of a (hypercubic) lattice of N spins ($s_i=\pm 1$), which may point up ($s_i=+1$) or down ($s_i=-1$). Spins are coupled to nearest neighbors (through a ferromagnetic exchange interaction J), and to an external field $H(t)$ that is increased adiabatically slowly. To model dirt in the material, we assign a random field h_i to each spin, chosen from a distribution $P(h_i)=\exp(-h_i^2/2R^2)/\sqrt{2\pi}R$, where R, the disorder, determines the width of the Gaussian probability distribution and, therefore, gives a measure of the amount of quenched disorder for the system.

The Hamiltonian for the system at a time t is given by $H=\Sigma_{\langle ij\rangle}-Js_is_j-\Sigma_i[H(t)+h_i-J_{inf}M]s_i$, where J_{inf} is the strength of the infinite range demagnetizing field ($J_{inf}=0$ for the nucleation model), $M=(1/N)\Sigma_i s_i$ is the magnetization of the system, and $\langle ij\rangle$ stands for nearest neighbor pairs of spins. Initially, $H(-\infty)=-\infty$ and all the spins are pointing down. Each spin is always aligned with its local effective field $h_i^{eff}=J\Sigma_{\langle ij\rangle}s_j+H(t)+h_i-J_{inf}M$. The external field $H(t)$ is adiabatically slowly increased from $-\infty$ until the local field h_i^{eff} of any spin s_i changes sign, causing the spin to flip [8,10]. It takes some microscopic time Δt for a spin to flip ($\Delta t\equiv 1$ for our simulation). The spin flip changes the local field of the nearest neighbors and may cause them to flip as well. This *avalanche* process continues until no more spin flips are triggered. Each step of the avalanche, that is, each Δt in which a set of spins simultaneously flip, is called

a *shell*. The number of spins that flip in a shell is directly proportional to the voltage $V(t)$ during the interval Δt that an experimentalist would measure in a pickup coil wound around the sample. In our simulations we, therefore, denote the number of spins flipped in a shell at a time t by $V(t)$. The first shell of an avalanche (one spin flip) is triggered by the external field $H(t)$, while each subsequent shell within the avalanche is triggered only by the previous shell, since $H(t)$ is kept constant while the avalanche is propagating. $H(t)$ is only increased when the current avalanche has stopped, and is increased only until the next avalanche is triggered (i.e., $dH/dt \to 0$). The number of shells in an avalanche times Δt defines the *pulse duration* T or the time it took for the entire avalanche to flip. In this paper we will be interested in looking at $V(t,T)$ for $0<t\leqslant T$, that is, the voltage as a function of time for an avalanche of a given duration T.

The front propagation model exhibits self-organized criticality (SOC) [11–13]. This means that as H is increased the model always operates at the critical depinning point, and no parameters need to be tuned to exhibit critical scaling behavior (except $dH/dt \to 0$). The nucleation model, on the other hand, is a plain old critical system with a continuous second order phase transition with disorder as the tuning parameter. The continuous nonequilibrium phase transition can be understood as follows. For zero disorder, the random fields of each spin will be the same, so that when one spin is flipped the entire lattice of spins will flip. This results in a rectangular hysteresis curve with a macroscopic jump in the magnetization when the external field overcomes the interaction with the neighbors. On the other hand, if the disorder is infinite, each spin will have a very different random field, so as when the external field is raised each spin will essentially flip independently, triggering no other spins to flip. This will result in a smooth ''hysteresis'' curve with an approximately constant slope [$M(H) \sim H$ over a wide range of H]. In between these two phases of behavior there is a continuous phase transition at some critical value $R=R_c$. At the transition each branch of the hysteresis loop has a single point with infinite slope ($dM/dH|_{\pm H_c} \to \infty$) at a critical field $H=\pm H_c$. R_c and H_c are nonuniversal. In three dimensions they are $R_c=2.16$ and $H_c=1.43$ (in units of J) [14]. The transition is characterized by a number of universal critical exponents [15], and scaling functions. In this paper we specifically focus on only two exponents: $1/\sigma\nu z$ and τ, and one scaling function. The significance of these exponents is given later. The scaling function we examine can be obtained through experiment as well as simulation. Details of the simulation algorithm are given elsewhere [16].

III. THE EXPERIMENTS

In addition to examining results obtained from simulation we study results from three different experiments. We performed one of these experiments, and the results for the other two experiments were obtained from already published results [17,18].

Our own experiment was performed on an (unstressed) amorphous alloy, $Fe_{21}Co_{64}B_{15}$. The data we present from Durin and Zapperi [18] is from an experiment on an amorphous alloy with a different composition, $Fe_{64}Co_{21}B_{15}$, under a tensile stress. Studies of the effect of tensile stress on samples of this type indicate that for low tensile stress, the domain structure is a complicated pattern of maze domains, dominated by quenched-in stresses [19]. On the other hand, when such materials undergo tensile stress, the uniaxial anisotropy gives way to a simpler domain structure with a few parallel domains in the direction of the stress [19]. Related to this change in domain structure is a change in the dominant interaction in the material. In amorphous alloys under stress, surface tension effects are thought to be more important than dipolar interactions, while dipolar interactions dominate for polycrystals and materials with small grains [20].

Durin and co-workers sample was under stress so as to enhance stress-induced anisotropy so much that the long range dipolar interactions can be neglected, placing their experiment into the universality class of the front propagation model [20,22,23]. Sample of Spasojević *et al.* was a quasi-two-dimensional metal glass, more precisely a commercial VITROVAC 6025 X [17]. Based on the scaling exponents obtained from the experiment of Spasojević *et al.* (given later), their experiment does not seem to fall into any universality class discussed in this paper. Our experiment seems to be in a crossover regime between two universality classes; details are given later in this paper. Further details about the experiments of Durin and co-workers and Spasojević *et al.* experiment can be obtained elsewhere [17–20].

IV. EXTRACTING PULSE SHAPES

Nucleation model. We simulate four realizations of a 1200^3 system near $R=R_c$ ($R=2.2$) and record the time series $V(t,T)$ of avalanches from an H window near H_c ($1.42<H<1.43$). We average avalanches of a fixed pulse duration T (within the interval $[T,1.05T]$), for various values of T. In each case we average over 1000–2000 avalanches to ensure strong fluctuations have been averaged out. We check finite size effects by performing simulations at 800^3 and 1000^3 and verifying that identical avalanche shapes (within small fluctuations) are obtained for all system sizes.

Front propagation model. We perform 100 realizations of a 400^3 system and record avalanches from an H window within the slated part of the hysteresis loop ($1.25<H<1.88$). Even though the front propagation model exhibits SOC due to the infinite-range demagnetizing interaction, in order to avoid effects due to initial nucleation of the front (beginning of the hysteresis loop), or when the front encounters the boundaries of the simulation (the end of the hysteresis loop) we must choose avalanches near the middle of the hysteresis loop. We obtain avalanche shapes $V(t,T)$ in a manner identical to how they were obtained for the nucleation model. We check finite size effects by performing simulations of 200^3 and 300^3 size systems, and find a consistent avalanche shape for all three system sizes.

Experiment. Measurements were performed on a 21 cm $\times$ 1 cm $\times$ 30 μm ribbon of $Fe_{21}Co_{64}B_{15}$ alloy, a soft amorphous ferromagnet obtained from Gianfranco Durin. A solenoid, driven with a triangle wave, applies a magnetic field along the long axis of the sample. Since domain wall motion

dominates over other means of magnetization in the linear region of the loop, data were collected in only a selected range of applied fields near the center of the loop. The Barkhausen noise was measured by a small pickup coil wound around the center of the sample. This voltage signal was amplified, antialias filtered and digitized, with care taken to avoid pickup from ambient fields. Barkhausen noise was collected for both increasing and decreasing fields for 80 cycles of the applied field through a saturation hysteresis loop. The driving frequency was 0.01 Hz; this corresponds to $c=0.09$, where c is a dimensionless parameter proportional to the applied field rate and is defined in the Alessandro Beatrice Bertotti Montorsi model (ABBM model) for the Barkhausen effect [24]. In this way, our measurements should be well inside the $c<1$ regime identified in the ABBM model, in which we can expect to find separable avalanches rather than continuous domain wall motion.

Due to background noise in real experimental data there is no definitive way to determine when an avalanche begins and when one ends; we set a sensitivity threshold that is high enough to cut out background noise and low enough to capture enough of the avalanche so as not to affect the shape. We check the validity of our threshold by perturbing the threshold by a small amount and noticing that there is no change in the avalanche shape.

V. CRITICAL EXPONENTS AND DATA COLLAPSES

In the front propagation model, as well as in the nucleation model near (R_c, H_c), the voltage $V(T,t)$ scales as [8]

$$V(T,t)=T^{1/\sigma\nu z-1}f_{shape}(t/T). \tag{1}$$

By collapsing average avalanche shapes of various durations T we determine the universal scaling function, $f_{shape}(t/T)$, and the critical exponent $1/\sigma\nu z$. The exponent $1/\sigma\nu z$ relates the avalanche size S to the avalanche pulse duration T at criticality by $S\sim T^{1/\sigma\nu z}$. We find that the critical exponent $1/\sigma\nu z$ for the front propagation and nucleation model, obtained from simulation, is in close agreement with previous theoretical predictions and with experimental values [25]. The collapses are shown in Figs. 1 and 2.

We also determine the avalanche size distribution that scales as $D(S)\sim S^{-\tau}$ at criticality. The avalanche size distributions for our simulation and our experiment are given in Fig. 3; the values obtained for τ, for the front propagation model and nucleation model, are in close agreement with previously quoted values [8,14]. Experimentally, the scaling exponent τ weakly depends on c in some materials [19]. From this dependence we find that there may be a difference of 0.02 between the value of τ we find in our experiment and the value of τ at $c=0$ (zero frequency). However, this difference is within the error bars we give for τ. Table I summarizes results for τ and $1/\sigma\nu z$ for experiment, simulation, and mean field theory (MFT). We see that the critical exponents for the front propagation model agree (within error bars) with exponents from experiment of Durin *et al.*, as expected.

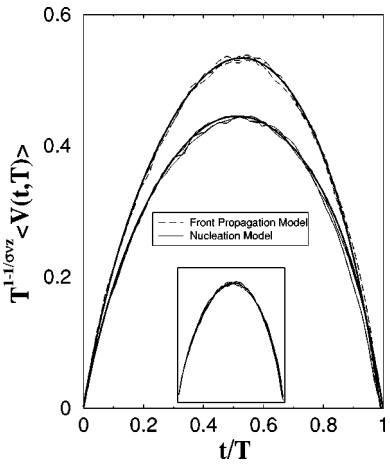

FIG. 1. Pulse shape collapses of $V(t,T)$ (the number of spins flipping in each time step) obtained from simulation. Three pulse shapes were collapsed for each model; these pulse shapes represent averaged avalanches of pulse durations $T=52$, 73, and 106 (total number of time steps) within 5%. From the collapse of front propagation model avalanche pulse shapes, we find $1/\sigma\nu z=1.72\pm0.03$. From the collapse of nucleation model avalanche pulse shapes, we find $1/\sigma\nu z=1.75\pm0.03$. The bold line going through the collapses is the nonlinear curve fit obtained from the set of orthonormal polynomials presented in this paper [Eqs. (2)–(6)]. Note that the nonlinear curve fit is shown for only one of the collapsed averaged avalanches in each case. Inset: By rescaling the height of the nucleation model collapse by 20% we obtain a collapse of pulse shapes from the two different models suggesting that their pulse shapes are very similar, but quantitatively not the same as described in the text.

While the Durin and Zapperi experiment is believed to fall into the front propagation universality class, as discussed above, our experiment is neither in the front propagation nor in the mean field universality class. *A priori* we would assume that our experiment would be in the mean field universality class since our sample was unstressed, and previous experiments have indicated that unstressed samples will exhibit mean field behavior [20]. The critical exponents found from our experiment indicate that it maybe in a crossover regime between the mean field and the front propagation universality classes. The exponent τ has a value of 1.46 ± 0.05 (see also Table I), which is between the value of 1.28 for the front propagation model (sample with stress) and the mean field value of 1.5 (sample without stress) [8,20]. In addition, the exponent $\alpha=1.74\pm0.06$, determined from the avalanche pulse duration distribution given by $D(T)\sim T^{-\alpha}$ at criticality, (see inset of Fig. 2), is between the value of 1.5 for the front propagation model (with stress), and the mean field value of 2 (without stress) [18]. Residual stress on our sample may have resulted in these anomalous exponents.

Although our experiment may be in a crossover regime, we were able to obtain a good collapse of the avalanche pulse shapes (see Fig. 2). In order to reaffirm the validity of the exponent obtained from the collapse, we independently checked the value of $1/\sigma\nu z$ from the power spectra [$P(w)\sim w^{-1/\sigma\nu z}$ at criticality], and found $1/\sigma\nu z=1.73\pm0.08$, which is consistent (within errors bars) with $1/\sigma\nu z=1.70\pm0.05$ obtained from the experimental avalanche pulse collapse.

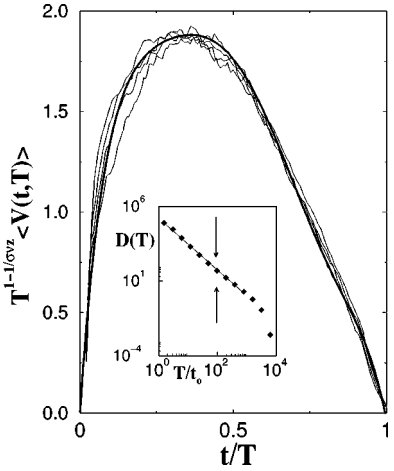

FIG. 2. Collapse of averaged experimental avalanche pulse shapes $\langle V(t,T)\rangle$ (in units of 0.316 mV) is shown, yielding $1/\sigma\nu z = 1.70 \pm 0.05$. The four curves represent averaged avalanches of pulse duration: $T = 88t_o$, $110t_o$, $132t_o$, and $165t_o$ within 10%, where $t_o = 6.4$ μs represents the time between each measurement of the Barkhausen noise train. Each of the four curves is an average of between 1152 to 1561 avalanches. The smooth bold curve is a fit of the averaged avalanche of duration $T = 132t_o$ using the orthonormal polynomials given in Eqs. (2)–(6). Inset: Pulse duration distribution $D(T)$ (number of pulses of duration T), obtained from our experiment. Avalanche pulse shapes were extracted from the region indicated by the arrows, and this region is well within the scaling regime. In this scaling regime $D(T)$ scales as $D(T) \sim T^{-\alpha}$ where $\alpha = 1.74 \pm 0.06$. This value of α is between the mean field value of $\alpha = 2.0$ (sample without stress) and the value of $\alpha = 1.5$ for front propagation dynamics (sample with stress) [20], indicating that our experiment may be in a crossover regime.

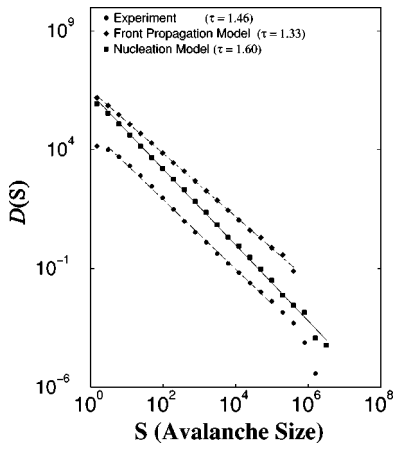

FIG. 3. Avalanche size distribution, $D(S)$ (number of avalanches of size S), for the front propagation model, the nucleation model, and our experiment. The exponent τ given in the legend is the critical exponent corresponding to the scaling of the avalanche size distribution $[D(S) \sim S^{-\tau}]$. For experiment S is given in units of 2.022 mV μs, for simulation S is the total number of spins flipped in an avalanche.

VI. FITTING TO ORTHONORMAL POLYNOMIALS

The mean field shape of avalanches in our model $V^{MFT}(t,T)$ is an inverted parabola [21]. In order to study corrections to the mean field shape, in simulation and experiment, we derive a set of orthonormal polynomials $f_i(t)$ with $f_i(-L) = f_i(L) = 0$, where $L = T/2$ is half the duration of the avalanche. The negative of the first polynomial $f_0(t)$ is proportional to the mean field result. The first five polynomials of the set are

$$f_0(t) = \sqrt{\frac{15}{16L^5}}(t^2 - L^2), \tag{2}$$

$$f_1(t) = \sqrt{\frac{105}{16L^7}}(t^3 - L^2 t), \tag{3}$$

$$f_2(t) = \sqrt{\frac{45}{64L^9}}(7t^4 - 8L^2t^2 + L^4), \tag{4}$$

$$f_3(t) = \sqrt{\frac{1155}{64L^{11}}}(3t^5 - 4L^2t^3 + L^4 t), \tag{5}$$

$$f_4(t) = \sqrt{\frac{1365}{2048L^{13}}}(33t^6 - 51L^2t^4 + 19L^4t^2 - L^6). \tag{6}$$

We fit a linear combination of the above polynomials to the average avalanche shape obtained from simulation and experiment. L is also left as a free parameter in the fits to the average shapes. The pulse duration is then precisely defined as $T = 2L$. The results of the fits are shown in Figs. 1 and 2. In Fig. 4 we give the coefficients for the fits, found in simulation and experiment. We also include the coefficients for the fit to an average avalanche shape determined by experiment of Durin and Zapperi [18], whose avalanche shape is given in Fig. 5. The coefficients are determined from the total fit function,

$$F(t) = a_0 f_0(t) + a_1 f_1(t) + a_2 f_2(t) + a_3 f_3(t) + a_4 f_4(t), \tag{7}$$

where a_0, a_2, and a_4 are the *symmetric* coefficients of the fit, while a_1, a_3 are the *antisymmetric* coefficients of the fit (i.e., multiplying polynomials that are not symmetric under time reversal $t \to -t$). We are particularly interested in the asymmetry of the avalanche shapes.

From inspection of the avalanche shapes we see that the experimental avalanche shapes are strongly asymmetric under time reversal, while the avalanche shapes determined from the simulation of the two models are both very close to symmetric. Quantitatively, the coefficients for the avalanche shapes of the nucleation model are very similar to those of the front propagation model and both are different from the coefficients of experimental avalanche shapes. While avalanche shapes in both models are slightly asymmetric to the left [i.e., $V(t,T)$ increases more slowly than it decreases], the experimental avalanche shapes are strongly asymmetric to the right direction [i.e., $V(t,T)$ increases quickly and decreases slowly]. The origin of this difference between theory

TABLE I. The critical exponents τ and $1/\sigma\nu z$ in $d=3$ dimensions for the nucleation model, front propagation model, and all three experiments discussed in this paper. We also include the mean field values of these exponents.

	Nucleation model	Front propagation model	Our experiment Durin *et al.* expt. [17] Spasojević *et al.* expt. [20,18]	Mean field [16]
	1.60 ± 0.04	1.33 ± 0.08	1.46 ± 0.05	
τ	1.60 ± 0.06 [14]	1.28 [16]	1.27 ± 0.03 [20,22] 1.77 [17]	1.5
	1.75 ± 0.03	1.72 ± 0.03	1.70 ± 0.05	
$1/\sigma\nu z$	1.75 ± 0.07 [14]	1.72 [16]	1.77 ± 0.12 [20,18] 1.58 [17]	2

and experiment is not yet understood. It comes as a surprise, since the critical exponents obtained in the experiment of Durin and co-workers are in close agreement with exponents obtained from the front propagation model (see Table I) and the avalanche shapes are expected to be just as universal as the critical exponents. On the other hand, we see in Fig. 5 that different experiments give different pulse shape scaling functions. This difference may be a result of the fact that the experiments are not in the same universality class. Nevertheless, all the experimental pulse shapes do have the same sign of asymmetry.

We did one check on whether the pulse shape function in our model is indeed *universal*, an assumption often taken for granted: We changed the lattice of our simulation from a simple cubic to a bcc (body centered cubic) lattice and found an identical pulse shape scaling function (within small statistical error), as expected when universality holds.

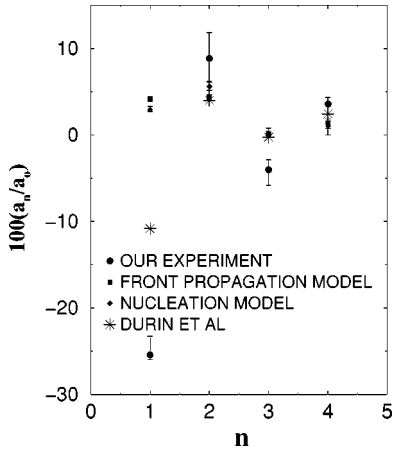

FIG. 4. Fitting coefficients to the avalanche shapes determined for the two models, our experiment, and the experiment of Durin and Zapperi [18]. We find that the coefficients are very similar for the two models. While the a_1 coefficients determined from the experiments are significantly different from the two models, the difference is not only in the sign of asymmetry but also in the magnitude of asymmetry. Each fitting coefficient, except for Durin and Zapperi, was determined from three realizations of the universal scaling function in each case. The coefficients, for the two models and our experiment, plotted above, represent median values, while the error bars are determined from the higher and lower values. Durin and Zapperi avalanche shape, presented in Fig. 5, was used to calculate the coefficients presented above; no error bars are provided in this case since only one realization was available.

VII. DISCUSSION AND CONCLUDING REMARKS

In performing these analyses we have stumbled upon an interesting observation: after appropriate rescaling of the y axis, the universal pulse shape function for the front propagation and nucleation model appear to look the same (see inset for Fig. 1) even though we know [7] that the models do not belong to the same universality class. However, upon more precise quantitative analysis we see that they are in fact different, their a_1 coefficients are different by several σ. Furthermore, we tried to collapse two pulse shape functions with $T\simeq52$ from the two different models and found that they could not be collapsed precisely despite, naturally, scaling by different critical exponents appropriate for the two models. The front propagation pulse scaling function is more asymmetric, as supported by the somewhat larger a_1 fit coefficient compared to the nucleation model result.

By examining the pulse shape scaling functions as a sharper test than merely critical exponents for the universal-

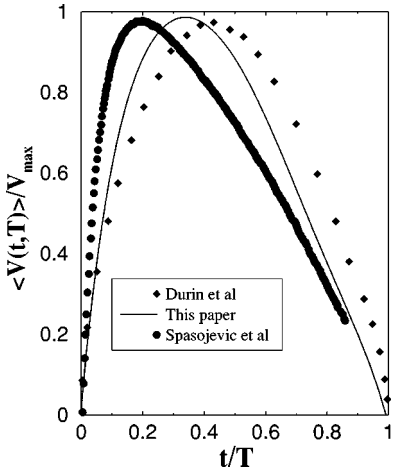

FIG. 5. Comparison of our experimental pulse shapes with experimental pulse shapes obtained by two other groups. The sample of Durin and co-workers was under stress with large stress induced anisotropies, putting their experiment into the universality class of front propagation [20,22,23]. For Durin's experiment $1/\sigma\nu z=1.77$ [18] and $\tau=1.27$ [20,22]. For Spasojević's experiment $1/\sigma\nu z=1.58$ and $\tau=1.77$ [17].

ity class of the nonequilibrium zero-temperature RFIM, we raised many questions. What accounts for the difference between theory and experiment, and between different experiments? Is the theory incomplete or inaccurate at this level of description? Experimentally, we do not yet know what material features are required to produce universality of the pulse shape function. Differences between experimental results make further experimental tests desirable (see Fig. 5).

Although the three experiments we examined do not fall into the same universality class and do not have very similar pulse shapes, they share one universal aspect not shared by the results from simulation: all the experimental averaged pulse shapes are asymmetric in the leftward direction. This suggests that there may be a phenomena that exists in real materials that has not been accounted for in theory.

ACKNOWLEDGMENTS

We would like to thank M. B. Weissman, G. Durin, A. Travesset, and R. A. White for very useful discussions. We also thank M. Kuntz and J. Carpenter for providing the front propagation model simulation code. K.D. and A.P.M. acknowledge support from NSF via Grant No. DMR 99-76550, the Materials Computation Center, through NSF Grant No. 99-72783, and from IBM, which provided the computers that made the simulation work possible. J.P.S. acknowledges support from NSF via Grant No. DMR 98-73214. A.C.M. acknowledges support from NSF via Grant No. DMR 99-81869. A.P.M. would also like to acknowledge the financial support provided by UIUC and K.D. gratefully acknowledges financial support from the Alfred P. Sloan Foundation.

[1] J. P. Sethna, J. D. Shore, and M. Huang, Phys. Rev. B **44**, 4943 (1991), and references therein; J. D. Shore, Ph.D. thesis, Cornell University, 1992, and references therein; T. Riste and D. Sherrington, in *Phase Transitions and Relaxation in Systems with Competing Energy Scales*, Vol. 415 of *NATO Advanced Study Institute, Series C: Mathematical and Physical Sciences*, edited by T. Riste and D. Sherrington (Geilo, Norway, 1993), and references therein; M. Mézard, G. Parisi, and M. A. Virasoro, *Spin Glass Theory and Beyond* (World Scientific, Singapore, 1987), and references therein; K. H. Fischer and J. A. Hertz, *Spin Glasses* (Cambridge University Press, Cambridge, 1993), and references therein; G. Grinstein and J. F. Fernandez, Phys. Rev. B **29**, 6389 (1984); J. Villain, Phys. Rev. Lett. **52**, 1543 (1984); D. S. Fisher, *ibid.* **56**, 416 (1986).

[2] S. Field, J. Witt, F. Nori, and X. Ling, Phys. Rev. Lett. **74**, 1206 (1995).

[3] W. Wu and P. W. Adams, Phys. Rev. Lett. **74**, 610 (1995).

[4] M. P. Lilly, P. T. Finley, and R. B. Hallock, Phys. Rev. Lett. **71**, 4186 (1993); A. H. Wooters and R. B. Hallock, Physica B **141**, 284 (2000).

[5] J. Ortín *et al.*, J. Phys. IV **5**, 209 (1995).

[6] B. Gutenberg and C. F. Richter, Ann. Geofis. **9**, 1 (1956).

[7] J. P. Sethna, K. A. Dahmen, and C. R. Myers, Nature (London) **410**, 242 (2001).

[8] Matthew C. Kuntz and James P. Sethna, Phys. Rev. B **62**, 11 699 (2000).

[9] J. P. Sethna, K. Dahmen, S. Kartha, J. A. Krumhansl, B. W. Roberts, and J. D. Shore, Phys. Rev. Lett. **70**, 3347 (1993).

[10] James P. Sethna, Olga Perković, and Karin A. Dahmen, e-print cond-mat/9704059.

[11] J. S. Urbach, R. C. Madison, and J. T. Markert, Phys. Rev. Lett. **75**, 276 (1995).

[12] O. Narayan, Phys. Rev. Lett. **77**, 3855 (1996).

[13] S. Zapperi, P. Cizeau, G. Durin, and H. E. Stanley, Phys. Rev. B **58**, 6353 (1998).

[14] Olga Perković, Karin A. Dahmen, and James P. Sethna, Phys. Rev. B **59**, 6106 (1999).

[15] Olga Perković, Karin Dahmen, and James P. Sethna, Phys. Rev. Lett. **75**, 4528 (1995).

[16] Matthew C. Kuntz, Olga Perković, Karin A. Dahmen, Bruce W. Roberts, and James P. Sethna, Comput. Sci. Eng. **1**, 73 (1999).

[17] Djordje Spasojević, Srdjan Bukvić, Sava Milošević, and H. E. Stanley, Phys. Rev. E **54**, 2531 (1996).

[18] G. Durin and S. Zapperi, e-print cond-mat/0106113.

[19] G. Durin and S. Zapperi, J. Appl. Phys. **85**, 5196 (1999).

[20] G. Durin and S. Zapperi, Phys. Rev. Lett. **84**, 4705 (2000).

[21] Matthew C. Kuntz and James P. Sethna (private communication).

[22] G. Durin (private communication).

[23] H. Ji and M. O. Robbins, Phys. Rev. B **46**, 14 519 (1992).

[24] B. Alessandro, C. Beatrice, G. Bertotti, and A. Montorsi, J. Appl. Phys. **68**, 2901 (1990).

[25] K. A. Dahmen, Ph.D. thesis, Cornell University, 1995.